Letter Vol. 44, No. 17 / 1 September 2019 / Optics Letters 4115

Optics Letters

Efficient nonlinear compression of a mode-locked thin-disk oscillator to 27 fs at 98 W average power

Chia-Lun Tsai,[1,*] Frank Meyer,[2] Alan Omar,[2] Yicheng Wang,[2] An-Yuan Liang,[1] Chih-Hsuan Lu,[1] Martin Hoffmann,[2] Shang-Da Yang,[1] and Clara J. Saraceno[2]

[1]Institute of Photonics Technologies, National Tsing Hua University, Hsinchu 30013, Taiwan
[2]Photonics and Ultrafast Laser Science, Ruhr University Bochum, Bochum, Germany
*Corresponding author: s102066805@m102.nthu.edu.tw

Received 17 May 2019; revised 16 July 2019; accepted 16 July 2019; posted 22 July 2019 (Doc. ID 367737); published 21 August 2019

We demonstrate efficient pulse compression of a 13.4 MHz, 534 fs, 123 W, Yb:YAG thin-disk oscillator down to 27 fs at 98 W average power, resulting in a record-high 166 MW peak power from an amplifier-free oscillator-driven setup. Our compressor is based on two stages: one multipass cell allowing us to reduce the pulse duration to sub-90 fs and, subsequently, a multiple-plate compressor, allowing us to reach 27 fs. The overall average power compression efficiency is 80%, and the beam has excellent beam quality and homogeneity. In addition, we demonstrate further spectral broadening that supports a transform limit of 5 fs in a second multiple-plate stage, demonstrating the potential for reaching a 100 W class, amplifier-free, few-cycle source in the near future. The performance of this unique source is very promising for applications previously restricted to amplified sources, such as efficient generation of extreme ultraviolet light at high repetition rate, and the generation of high-power broadband THz radiation.

https://doi.org/10.1364/OL.44.004115

High average power ultrafast lasers based on Yb-doped materials have seen spectacular progress in the last few years. Nowadays, kilowatt average powers in various architectures (slabs, disks, and fibers) with pulse energies ranging from tens of μJ at multi-megahertz (MHz) repetition rates to several hundreds of millijoules at kilohertz (kHz) repetition rate have been demonstrated, and no show-stoppers appear to hinder further progress.

Ultrafast thin-disk lasers (TDLs) have consistently been at the forefront of this progress. Among the different ultrafast disk architectures, mode-locked thin-disk oscillators are particularly attractive for applications requiring very high repetition rates (MHz and beyond) at highest pulse energies. Average powers of several hundreds of watts and pulse energies approaching 100 μJ [1] have been demonstrated, reaching comparable performance to their amplifier counterparts, but from a simple amplifier-free, one-box oscillator, delivering potentially lowest noise levels from transform-limited (TL), soliton-shaped pulses. Examples of areas where such compact high-power femtosecond (fs) oscillators could have profound impact are for the generation of high-flux extreme ultraviolet (EUV) radiation for attosecond spectroscopy, for EUV frequency comb spectroscopy, or for high-power broadband terahertz (THz) time-domain spectroscopy.

However, so far, applications of this promising technology in scientific areas remain widely unexplored, mostly because of the rather long pulse duration obtained directly from Yb-based ultrafast lasers. In fact, most experiments in the aforementioned areas require not only highest possible pulse energy and high repetition rate, which are readily available, but also critically rely on short pulse durations (<30 fs down to single-cycle). Whereas reaching this performance directly from a high average power oscillator is an active area of research, a trade-off between pulse duration and average power and pulse energy is so far unavoidable. For example, sub-100 fs pulses are rarely reached with >10 W average power and >1 μJ pulse energy, and sub-50 fs pulses have only been achieved with <2 W [2,3]. So far, no mode-locked TDL has been demonstrated with <30 fs.

An alternative approach to reach the desired regime is to use external pulse compression via nonlinear spectral broadening and consequent dispersion compensation. State-of-the-art pulse peak powers from mode-locked TDLs are in the order of tens of MW; therefore, we restrict our discussion to recent compression results with input peak powers above the self-focusing critical power in fused silica (FS) (approximately 4 MW), which are most relevant to the latest obtained results.

One suitable technique for this parameter regime is spectral broadening in gas-filled Kagome-type hollow-core fibers [4,5], which offer large flexibility due to the gas-filled core. However, fiber coupling in these fibers is technically very challenging at high average power [5], requiring excellent beam quality and stable beam pointing at the input of the fiber to prevent damage and obtain a stable output. Furthermore, these fibers require extremely cautious mounting for average power handling and can suffer from gas-induced depolarization [6].

In this regard, solid-state techniques are preferred for their simplicity and reliability, but potential spatial–temporal couplings and resulting beam degradation need to be carefully controlled. Both multipass cells [7,8] and the multiple plate technique [9] have recently emerged as promising methods to overcome this limitation, by enabling spatially homogeneous spectral broadening while keeping the B-integral per pass (or per plate) sufficiently low.

In their very early realizations, multipass cells with FS as the nonlinear medium have very successfully confirmed their potential for compression of high-average power, μJ-level pulses from Innoslab amplifiers [10], where 860 fs pulses with approximately 8 MW peak power were compressed to 115 fs at 300 W of average power and 7.5 μJ pulse energy. More recently, they have been used to compress Kerr-lens mode-locked (KLM) TDLs. In [11], pulses from a 15.6 MHz repetition rate, KLM-TDL with 80 W of average power (5.1 μJ pulse energy) and 190 fs pulse duration (24 MW peak power) were compressed to 40 fs with a resulting peak power of 67 MW and 94% efficiency. Reaching sub-30 fs is, however, difficult to achieve with a single multipass cell stage due to the limited degrees of freedom in dispersion management, thus requiring several subsequent stages, which increases complexity and reduces efficiency [12,13].

The multiple-plate technique is ideally suited to complement multipass cells in a simple, high-throughput (up to 88% [14]) setup with significantly higher flexibility, simplicity, and cost-efficiency to reach the single-cycle regime. This technique has been successfully applied to a wide range of pulse energies (from 54 μJ to >1 mJ) and average powers (up to 20 W at 50 kHz repetition rate [15]) and in various wavelength regions to reach subcycle pulse durations [14,16,17]. However, except for some qualitative estimations [18], it remained unclear whether this technique was suited for MHz repetition rate systems with 100 W average power and few to tens of μJ pulse energy.

Here, we demonstrate that the combination of multipass cells and the multiple-plate technique are an extremely promising avenue to realize laser sources with hundreds of watts of average power and few-cycle pulse duration, bringing Yb-doped sources with traditionally long pulses into the few-cycle regime with high efficiency. First, using one multipass cell and one multiple-plate stage, we demonstrate pulse compression of a semiconductor saturable absorber mirror (SESAM)-mode-locked TDL delivering 123 W of average power, operating at 13.4 MHz repetition rate with 534 fs pulses down to 27 fs at 98 W of average power, resulting in an overall power compression efficiency of 80%. The final 27 fs pulses have a peak power of 166 MW, thus enhancing the peak power of our oscillator by an order of magnitude. The beam quality of the compressed beam is very good with an $M^2 < 1.2$, and good spectral homogeneity of the beam is shown. To the best of our knowledge, this is the highest peak power ever achieved with a MHz repetition rate, amplifier-free system. Furthermore, this is the first time that the multiple-plate technique has been applied to a 100 W class MHz source with sub-10 μJ input pulse energy, further confirming the versatility of this technique. Finally, we demonstrate further broadening supporting 5 fs TL pulses in a second multiple-plate setup, indicating few-cycle pulses are within reach.

The experimental setup is shown in Fig. 1. The laser system is a home-built SESAM mode-locked oscillator operating at a

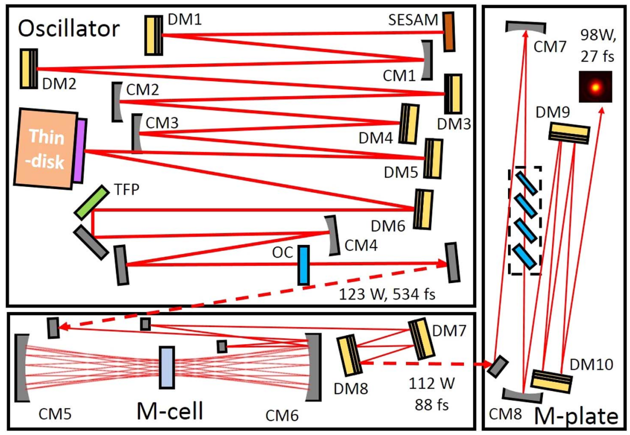

Fig. 1. Experimental setup: mode-locked thin-disk oscillator, multipass cell (M-cell), multiple-plate (M-plate) stage. DM#, dispersive mirror; CM#, curved mirror; TFP, thin-film polarizer; OC, output coupler. Near-field beam profile after compression is taken by a silicon-based CCD camera and shown in subset image.

central wavelength of 1030 nm and at a repetition rate of 13.4 MHz, which was described in more detail in [19]. The gain medium is a 100 μm, 10 at. % Yb-doped YAG disk, pumped by a volume Bragg grating stabilized diode laser emitting at 969 nm wavelength. Soliton mode locking is achieved by balancing the remaining air nonlinearity inside the resonator (operation at 35 mbar of air pressure) with $-6000\ \mathrm{fs}^2$ of intracavity group delay dispersion (GDD) per round trip. An intracavity thin-film polarizer is placed to ensure linear polarization at the output. Stable soliton mode locking is achieved up to 123 W (9.4 μJ pulse energy) at 400 W of pump power, at which point the pulses are nearly TL, with 534 fs duration. As expected from a TDL, the beam quality is excellent with a measured $M^2 < 1.1$ in both axes.

The oscillator seeds a first compression stage designed to reduce the pulse duration to sub-100 fs. The setup is based on the design presented in [10]. We use two concave mirrors with 300 mm radius of curvature (ROC) and separated by 540 mm that define a Herriott-type multipass cell. The oscillator beam is shaped to match the eigenmode of the cell using a reflective curved telescope. An antireflection (AR)-coated 12-mm-thick FS plate is placed at the focus to broaden the input spectrum via self-phase modulation over 42 passes, with a B-integral of $<0.4\pi$ per pass. The GDD induced by the plate is approximately compensated by one of the two concave mirrors of the cell, with a GDD of $-350\ \mathrm{fs}^2$. This configuration was chosen because numerical simulations showed optimal spectral broadening without beam quality degradation, in view of the available equipment at the time of the experiment. The spectrally broadened pulses are dechirped by 24 bounces on mirrors providing anomalous GDD of $-550\ \mathrm{fs}^2$ per reflection and are characterized by second-harmonic generation (SHG) frequency-resolved optical gating (FROG). The measured [Fig. 2(a)] and retrieved [Fig. 2(b)] FROG traces are in excellent agreement with a FROG error of 2×10^{-3}, using a 256×256 grid. Figure 2(c) shows the retrieved spectral intensity and phase. The excellent agreement between the spectral intensities retrieved by FROG (blue solid) and measured by an optical spectrum analyzer (OSA) (dashed) confirms the fidelity of

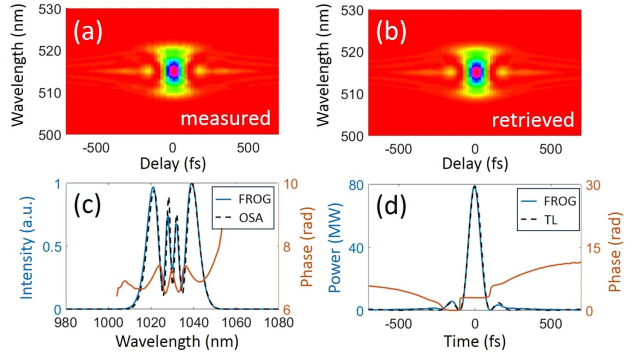

Fig. 2. Pulse characterization after first compression stage: (a) measured and (b) retrieved SHG-FROG traces. (c) Spectral intensity (blue solid line) and phase (brown solid line) by FROG retrieval. Power spectrum measured by an OSA (dashed line) is shown for comparison. (d) Temporal intensity (blue solid line) and phase (brown solid line) by FROG retrieval. Transform-limited (TL) temporal intensity (dashed line) is also provided as reference.

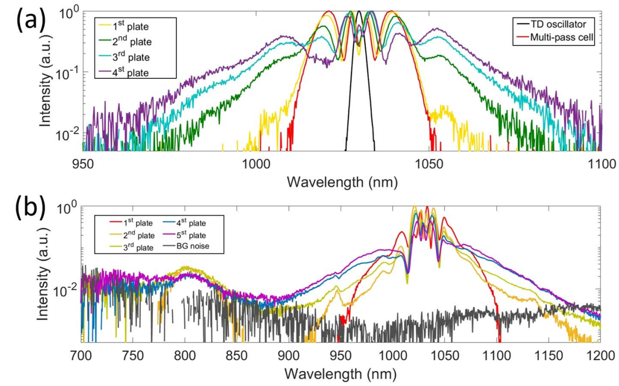

Fig. 3. (a) Power spectra measured after the thin-disk (TD) oscillator, multipass cell, and different numbers of thin plates in the multiple-plate stage. The observed symmetric broadening indicates self-phase modulation is the main broadening mechanism. (b) Power spectra measured after third broadening stage. BG noise, background noise.

the FROG reconstruction. In Fig. 2(d), the retrieved temporal intensity profile (blue solid) is nearly TL (dashed) and exhibits a duration at full width at half-maximum (FWHM) of 88 fs. The beam quality remains excellent with a measured $M^2 < 1.15$ (in both axes). After this first compression stage, the available average power is 112 W, resulting in a peak power of 80 MW. The overall compression efficiency of the first stage is 91% with the small loss mainly caused by the multiple reflections on the AR-coated FS plate.

The second compression stage is based on the multiple-plate technique consisting of four FS plates with 1 mm, 2 mm, 2 mm, and 3 mm thicknesses, placed at Brewster angle. A combination of concave mirrors results in a loose focus ($z_R = 15.9$ mm), a peak intensity of 1.2 $\mathrm{TW/cm^2}$ on the first plate, and a B-integral equals to 0.5π. The following plates are placed one after another to maximize spectral broadening without multiple filaments or laser-induced optical damage to the plate. When propagating through the plates, the pulses are also slightly temporally broadened due to material dispersion. As a result, the second, third, and fourth plates are increasingly thicker, but are placed after the real focal planes to approximately maintain the corresponding B-integral. The distances between adjacent plates is approximately 12 mm. Figure 3(a) shows the spectral intensity measured at the output of the thin-disk oscillator (black), multipass cell (red), and after each plate in the multiple-plate stage. The spectra are measured using an integrating sphere to provide spatially averaged results, which cancels uncertainties related to small spatial inhomogeneities of the beam (to be commented on in more detail below). The final spectrum spans 950–1100 nm (–20 dB), supporting 30 fs (FWHM) TL pulses.

Four bounces on dispersive mirrors with –200 $\mathrm{fs^2}$ GDD per reflection are used to compress the spectrally broadened pulses. Figure 4 shows the final compressed pulses after the entire two-stage compression setup, characterized by SHG FROG. We get excellent agreement between measured [Fig. 4(a)] and retrieved [Fig. 4(b)] FROG traces (FROG error is 4×10^{-3} at 512×512 grid) as well as good consistency between the power spectra obtained by FROG [blue solid, Fig. 4(c)] and OSA [black dashed, Fig. 4(c)]. The final compressed pulses have 27 fs duration (FWHM) and 166 MW peak power [blue, Fig. 4(d)]. Note that FWHM becomes a misleading metric in this case, where the TL pulse with the highest peak power (219 MW) corresponds to a broader FWHM value (30 fs). In our experiment, the TL peak power was not reached because of residual phase, which remained uncompensated by the dispersive mirrors available at the time of the experiment. The output power of the system was stable, with 0.6% fluctuation (root mean square value) measured over 170 min (102,000 data points).

The beam quality of the compressed pulses shown here is excellent with a measured $M_x^2 = 1.13$ and $M_y^2 = 1.40$. The small degradation observed in the y direction was attributed to the wedged plates (in the y direction) available at the time of the experiment. We verified this assumption by later replacing the plates with unwedged ones with same total thickness and observed an improvement in beam quality ($M_x^2 = 1.13$ and $M_y^2 = 1.24$). In this configuration, we characterized spectral homogeneity of our compressed beam using the approach

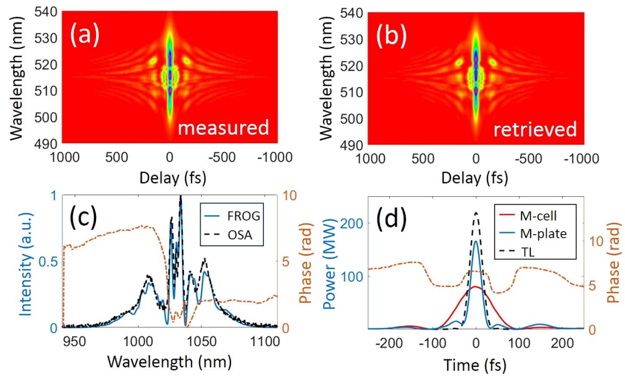

Fig. 4. Pulse characterization: (a) measured and (b) retrieved SHG-FROG traces. (c) Retrieved spectral intensity (blue solid) and phase (brown dotted). Power spectrum measured by OSA (dashed). (d) Temporal intensity (blue solid) and phase (brown dotted) by FROG retrieval. TL pulse (black dashed) and the pulse after the multipass cell compressor (red solid) are depicted as reference.

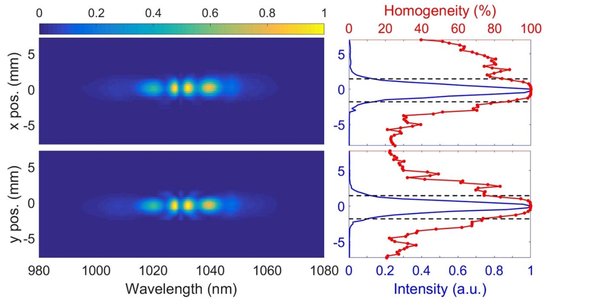

Fig. 5. Homogeneity measurement performed after multiple-plate stage supporting sub-30 fs. Dashed lines indicate $1/e^2$ level of intensity.

described in [10]. We measured 60 spectra along the x and y axes of the collimated beam after the plates without additional beam expansion (beam waist ω_{1/e^2} is 1.6 mm) using a single-mode fiber (with ~6 μm mode field diameter) coupled to an OSA (left panel, Fig. 5). For every spatial coordinate, we calculate a homogeneity value V (right panel, Fig. 5) corresponding to the spectral overlap to the spectrum at the center of the beam [10]. We measure $V > 80\%$ within $1/e^2$, indicating good homogeneity within the main beam. Beyond $1/e^2$, the V-factor is a poor measure in our setup due to the high noise level at small intensity. We then evaluate an intensity-weighted average V_{avg}, which is a measure of the overall spatial–spectral homogeneity. We obtain 97% (x axis) and 96% (y axis) using the full beam and 97% (x axis) and 95% (y axis) using a 3.5 mm diameter iris. The small difference indicates small amount of conical emission, typically associated to this technique. We confirm this by measuring small loss (11%) and a negligible change in M^2 ($M_x^2 = 1.10$ and $M_y^2 = 1.16$ with iris, versus $M_x^2 = 1.13$ and $M_y^2 = 1.24$ for the full beam) when the iris is present. We would like to highlight that an imperfect beam homogeneity indicates the existence of a small uncertainty in the claimed peak power, which can only be quantitatively analyzed by sophisticated spatial–temporal measurements, to be carried out more thoroughly in a future study.

To demonstrate the potential for further broadening, we add another multiple-plate stage after our 27 fs source. Figure 3(b) shows our results, using five plates with thicknesses of 1 mm, 1 mm, 1 mm, 2.3 mm, and 2.3 mm and a B-integral of 1.3π at the first plate. The distances between adjacent plates are approximately 1.2 mm. The resulting spectral broadening supports a TL pulse duration of 5 fs duration. Further analysis of the beam quality and spatial inhomogeneities in this second stage is currently being carried out. Sufficiently broadband dispersive mirrors and spectral phase characterization setup were not available at the time of these results; therefore, the pulses were not further compressed. We expect compression of these pulses to sub-10 fs will result in gigawatt (GW)-class peak power in the near future.

In conclusion, we report on a powerful technique to efficiently compress high-repetition-rate, Yb laser systems with hundreds of watts to the sub-30 fs regime, based on the combination of a multipass cell compressor and the multiple-plate continuum technique. We temporally compress a 123 W, 13.4 MHz mode-locked TDL from 534 fs, 16 MW to 27 fs, 166 MW, at 98 W of average power, thus enhancing the peak power of our oscillator by over an order of magnitude. The performance in terms of peak power is a record high from an amplifier-free ultrafast laser. In the near future, we will use our 27 fs source for high-power broadband THz generation and will further compress the pulses into the few-cycle regime.

Funding. Ministry of Science and Technology, Taiwan (MOST 107-2112-M-007-006, MOST 108-2918-I-007-014); Alexander von Humboldt-Stiftung; Deutsche Forschungsgemeinschaft (DFG) (CRC/TRR196 (MARIE) for project C10, EXC-2033 project 390677874).

REFERENCES

1. C. J. Saraceno, F. Emaury, C. Schriber, A. Diebold, M. Hoffmann, M. Golling, T. Sudmeyer, and U. Keller, IEEE J. Sel. Top. Quantum Electron. **21**, 106 (2015).
2. C. Paradis, N. Modsching, V. J. Wittwer, B. Deppe, C. Krankel, and T. Sudmeyer, Opt. Express **25**, 14918 (2017).
3. N. Modsching, C. Paradis, F. Labaye, M. Gaponenko, I. J. Graumann, A. Diebold, F. Emaury, V. J. Wittwer, and T. Sudmeyer, Opt. Lett. **43**, 879 (2018).
4. F. Emaury, A. Diebold, C. J. Saraceno, and U. Keller, Optica **2**, 980 (2015).
5. K. F. Mak, M. Seidel, O. Pronin, M. H. Frosz, A. Abdolvand, V. Pervak, A. Apolonski, F. Krausz, J. C. Travers, and P. S. J. Russell, Opt. Lett. **40**, 1238 (2015).
6. D. Mayer, C. T. Matthaei, A. Heuer, and M. Gühr, J. Opt. **21**, 025503 (2019).
7. J. Schulte, T. Sartorius, J. Weitenberg, A. Vernaleken, and P. Russbueldt, Opt. Lett. **41**, 4511 (2016).
8. P. Russbueldt, J. Weitenberg, A. Vernaleken, T. Sartorius, and J. Schulte, "Method and arrangement for spectral broadening of laser pulses for non-linear pulse compression," U.S. patent US9847615B2 (14 May 2014).
9. C. H. Lu, Y. J. Tsou, H. Y. Chen, B. H. Chen, Y. C. Cheng, S. D. Yang, M. C. Chen, C. C. Hsu, and A. H. Kung, Optica **1**, 400 (2014).
10. J. Weitenberg, A. Vernaleken, J. Schulte, A. Ozawa, T. Sartorius, V. Pervak, H. D. Hoffmann, T. Udem, P. Russbuldt, and T. W. Hansch, Opt. Express **25**, 20502 (2017).
11. S. Grobmeyer, J. Brons, M. Seidel, and O. Pronin, Laser Photon. Rev. **13**, 1800256 (2019).
12. K. Fritsch, M. Poetzlberger, V. Pervak, J. Brons, and O. Pronin, Opt. Lett. **43**, 4643 (2018).
13. L. Lavenu, M. Natile, F. Guichard, X. Délen, M. Hanna, Y. Zaouter, and P. Georges, Opt. Express **27**, 1958 (2019).
14. C. H. Lu, W. H. Wu, S. H. Kuo, J. Y. Guo, M. C. Chen, S. D. Yang, and A. H. Kung, Opt. Express **27**, 15638 (2019).
15. J. E. Beetar, S. Gholam-Mirzaei, and M. Chini, Appl. Phys. Lett. **112**, 051102 (2018).
16. P. C. Huang, C. Hernandez-Garcia, J. T. Huang, P. Y. Huang, C. H. Lu, L. Rego, D. D. Hickstein, J. L. Ellis, A. Jaron-Becker, A. Becker, S. D. Yang, C. G. Durfee, L. Plaja, H. C. Kapteyn, M. M. Murnane, A. H. Kung, and M. C. Chen, Nat. Photonics **12**, 349 (2018).
17. S. I. Hwang, S. B. Park, J. Mun, W. Cho, C. H. Nam, and K. T. Kim, Sci. Rep. **9**, 1613 (2019).
18. M. Seidel, G. Arisholm, J. Brons, V. Pervak, and O. Pronin, Opt. Express **24**, 9412 (2016).
19. F. Meyer, N. Hekmat, S. Mansourzadeh, F. Fobbe, F. Aslani, M. Hoffmann, and C. J. Saraceno, Opt. Lett. **43**, 5909 (2018).